



Hydrogen peroxide thermochemical oscillator as driver for primordial RNA replication

Rowena Ball and John Brindley

bioRxiv first posted online March 17, 2014

Access the most recent version at doi: <http://dx.doi.org/10.1101/003368>

**Creative
Commons
License**

The copyright holder for this preprint is the author/funder. It is made available under a [CC-BY-NC-ND 4.0 International license](#).

Hydrogen peroxide thermochemical oscillator as driver for primordial RNA replication

Rowena Ball

Mathematical Sciences Institute, The Australian National University, Canberra 0200, Australia

John Brindley

School of Mathematics, University of Leeds, Leeds LS2 9JT, U. K.

Abstract. This paper presents and tests a previously unrecognised mechanism for driving a replicating molecular system on the prebiotic earth. It is proposed that cell-free RNA replication in the primordial soup may have been driven by self-sustained oscillatory thermochemical reactions. To test this hypothesis a well-characterised hydrogen peroxide oscillator was chosen as the driver and complementary RNA strands with known association and melting kinetics were used as the substrate. An open flow system model for the self-consistent, coupled evolution of the temperature and concentrations in a simple autocatalytic scheme is solved numerically, and it is shown that thermochemical cycling drives replication of the RNA strands. For the (justifiably realistic) values of parameters chosen for the simulated example system, the mean amount of replicant produced at steady state is 6.56 times the input amount, given a constant supply of substrate species. The spontaneous onset of sustained thermochemical oscillations via slowly drifting parameters is demonstrated, and a scheme is given for prebiotic production of complementary RNA strands on rock surfaces.

Key words: RNA world; Thermochemical oscillator; Pre-biotic replication

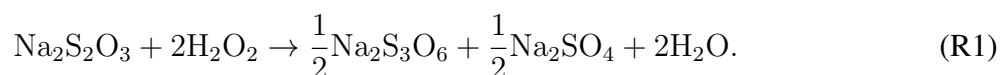
1. Introduction

Molecular self-replication is a fundamental process of all living organisms, and its initiation in the environment provided by the early Earth must have been essential for the emergence of life itself. In modern cells DNA replication is accomplished isothermally at moderate temperatures by a working army of enzymes using the free energy of ATP hydrolysis, and the strongly driven nonequilibrium condition is maintained by respiration and ion transport across cell membranes. However in the primordial soup there were no cells and no protein enzymes. The ‘RNA world’ hypothesis holds that cell-free RNA communities grew on solid surfaces and replicated, before the evolution of DNA [1]. What energy source may have driven RNA replication in such an environment?

It does seem that thermal cycling would be required to drive RNA replication in the absence of cellular (or other) machinery, because heat is required to dissociate double-stranded or multiplex RNA and a cooler phase is necessary for replication and annealing, given a supply of substrate template. This fact is often overlooked in hypotheses about the origin of life, as pointed out by Kováč et al. [2]. Exponential replication of RNA duplexes, fed by hairpins derived from an alanine tRNA and driven by externally imposed thermal cycling between 10 and 40°C, was achieved by Krammer et al. [3]. They proposed that, in the primordial soup, thermal cycling may have been provided by laminar convection between hot and cold regions in millimetre-sized rock pores [4], and that the substrate oligonucleotides could be concentrated by thermophoretic trapping.

It has been suggested by Matatov [5] that chemical energy also may have played a role in prebiotic evolution, because, in the laboratory, heat liberated in the decomposition of aqueous hydrogen peroxide (H_2O_2) supported formation of amino acids from simpler precursors. In this work we propose that a natural mechanism for driving self-sustained thermal cycling is a thermochemical oscillator, and demonstrate in a specific case that the temperature cycling for driving the amplification of template RNA in environments where early life may have evolved can be provided by a thermochemical oscillator driven by exothermic reactions of H_2O_2 .

Exothermic reactions of aqueous H_2O_2 are well-known to give rise to robust, self-sustained thermochemical oscillations with frequencies around $0.02\text{--}0.005\text{ s}^{-1}$ [6–9]. As our specific example we have chosen, with some justification expressed below, the oxidation of thiosulfate ion ($\text{S}_2\text{O}_3^{2-}$) by H_2O_2 , which is fast and highly exothermic:



The thermokinetics and thermochemistry of (R1) have been well-studied, and experimental data from the literature are collected in table 1. The reaction is first order in both reactants.

Oscillatory thermoconversion is typical of highly energetic, thermally sensitive, liquids such many of the peroxides [10]. The physical basis is as follows: In such liquids (and also in some vapor and gas phase substances), which have high specific heat capacity, the heat of reaction can be absorbed by the many intermolecular vibrational modes and intramolecular rotational modes. So the temperature rises but slowly as reaction proceeds, until these modes become saturated and consequently the temperature spikes — the heat cannot be absorbed any more by quantized excitations. But locally the reactant is depleted, so the temperature falls to a minimum before

Table 1. Experimental data for reaction (R1), presented in chronological order.

A ($\text{l mol}^{-1}\text{s}^{-1}$)	E (kJ/mol)	$-\Delta H$ (kJ/mol)	Ref.
6.85×10^{11}	76.52	573.0	[11]
2.13×10^{10}	68.20	585.8	[12]
7.33×10^{11}	78.24	594.1	[13]
1.63×10^{10}	68.12	612.5	[7]
6.8×10^{11}	77.0	not measured	[14]
2.00×10^{10}	68.20	586.2	[15]
2.0×10^{10}	68.3	562.8	[16]

reactant accumulation allows reaction to occur and heat to be released, and the cycle begins again. With a steady supply of reactant these self-sustained thermal oscillations can continue indefinitely.

1.1. H_2O_2 and thiosulfate on the early earth

One school of thought holds that the geochemical environment for the emergence of life was provided by submarine hydrothermal systems and hot springs [17]. Experiments reported by Foustoukos et al. [18] strongly support the conjecture that H_2O_2 is produced near hydrothermal vents when oxygenated seawater mixes with vent fluid.

Another source of H_2O_2 production in such an environment involves a surface reaction of pyrite (FeS_2) with H_2O and in experiments $0.391\text{--}0.567 \text{ mM/m}^2$ was produced [19, 20]. The specific surface area of pyrite is $2.0\text{--}4.0 \text{ m}^2/\text{g}$ [21], so there is a very real possibility that high concentrations of H_2O_2 could build up locally and be supplied at a constant rate for long periods of time. A very credible body of work (see references in [19]) holds that the most primitive photosynthetic cells used H_2O_2 as an electron donor, so it is reasonable to assume that H_2O_2 was produced long before those organisms evolved. Moreover it is believed that pyrite was present on the early earth. On the modern earth, pyrite deposits associated with hydrothermal activity can reach thicknesses of tens to hundreds of meters and spread over thousands of square kilometers within the crust [22].

Prebiotic production of H_2O_2 also may have occurred by photochemical disproportionation of the superoxide radical (O_2^-) in sunlit waters to H_2O_2 [23].

Thiosulfate ion is observed to occur in hydrothermal waters of Yellowstone National Park [24], so it is reasonable to conjecture that it was present in hydrothermal environments on the early earth.

Porous rocks around hydrothermal vents therefore could provide microenvironments where naturally self-sustaining thermochemical oscillations may be set up — namely, a localized, nonequilibrium forced flow system, and a supply of H_2O_2 and thiosulfate ion. If a supply of RNA oligonucleotides, perhaps synthesized on and dislodged from pore surfaces [25], is added to this recipe for primordial soup, replication may be driven by thermochemical temperature cycling.

2. Model, data and methods

For the reactive system in a single rock pore we employ a spatially homogeneous flow model; in other words, a continuous stirred tank reactor (CSTR) paradigm. An *a posteriori* assessment of

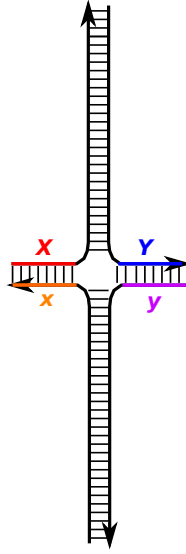


Figure 1. The quadruplex RNA species Z . The duplex replicator species are XY and xy , which for the purposes of the simulation are equivalent. See ref. [3] for more details. (Online version in colour.)

the rationale and validity of this model is given in section 4.1. The following dynamical system models the coupled evolution of the reactant concentrations in (R1) and the temperature:

$$V \frac{dc_v}{dt} = -V k_1(T) c_v c_w + F(c_{v,f} - c_v) \quad (1)$$

$$V \frac{dc_w}{dt} = -V 2k_1(T) c_v c_w + F(c_{w,f} - c_w) \quad (2)$$

$$V \bar{C} \frac{dT}{dt} = (-\Delta H_1) V k_1(T) c_v c_w - F \bar{C} (T - T_f) - L(T - T_a), \quad (3)$$

where the reaction rate constant $k_1(T) = A_1 \exp(-E_1/(RT))$, c_v is the concentration of thiosulfate and c_w is the concentration of H_2O_2 . The symbols and notation used in these and following equations are defined in table 2.

We used the following minimum subset of reactions from ref. [3] that can produce duplex RNA by autocatalysis:



where X and Y represent RNA complementary single-strands, the RNA duplex XY is the replicator and Z is the RNA quadruplex, the form of which is cartooned in figure 1. In the reaction

volume these species evolve as

$$V \frac{dc_{x+y}}{dt} = -V 2k_2(T) c_x c_y c_{xy} + F(c_{x,f+y,f} - c_{x+y}) \quad (4)$$

$$V \frac{dc_{xy}}{dt} = -V k_2(T) c_x c_y c_{xy} + V 2k_3(T) c_z + F(c_{f,xy} - c_{xy}) \quad (5)$$

$$V \frac{dc_z}{dt} = V k_2(T) c_x c_y c_{xy} - V k_3(T) c_z - F c_z, \quad (6)$$

where the notations c_{x+y} and $c_{x,f+y,f}$ are shorthand for $c_x + c_y$ and $c_{x,f} + c_{y,f}$, $k_2(T) = A_2 \exp(-E_2/(RT))$ and $k_3(T) = A_3 \exp(-E_3/(RT))$. (These are to be considered as empirical rate constants; (R2) as written is not intended to imply that an elementary three-body collision occurs.)

The enthalpy balance includes contributions from all reactions:

$$V \bar{C} \frac{dT}{dt} = (-\Delta H_1) V k_1(T) c_v c_w + (-\Delta H_2) V k_2(T) c_x c_y c_{xy} + (-\Delta H_3) V k_3(T) c_z - F \bar{C} (T - T_f) - L (T - T_a). \quad (7)$$

We derived the activation energies, pre-exponential factors, and reaction enthalpies from the rate data in [3], see the Appendix. Equations (1)–(3) (no RNA supply) and equations (1)–(2) and (4)–(7) (RNA single-strands and duplexes supplied), were integrated using a stiff integrator from reasonable initial conditions. The stability of steady state solutions was assessed over a range of the inflow temperature, T_f , by solving the corresponding eigenvalue problem and flagging points where an eigenvalue changed sign. These bifurcation points then were followed over a range of the thermal conductance L to obtain stability maps. Numerical values of the fixed parameters are given in table 2 and are discussed further in the Appendix.

3. Results

First we examined the behavior of the standalone H_2O_2 /thiosulfate system. Figure 2(a) shows the computed stability map. The régime of threefold multiplicity mapped by the locus of saddle-node bifurcations is included for completeness, but this régime is largely irrelevant for our purposes since the temperature is too low to drive RNA replication. At each point within the Hopf bifurcation loop the stable solution is a limit cycle. The time series for a selected point in the loop is shown in figure 2(b).

When reactions (R2) and (R3) are included, the stability map and temperature time series are indistinguishable numerically from those in figure 2 because the contributions of the second and third terms on the right hand side of equation (7) are relatively insignificant.

However, time series data rendered in figure 3 for the concentrations of single-strands, duplex, and quadruplex show that the H_2O_2 /thiosulfate thermochemical oscillator can indeed drive the RNA replication process. This time series was computed for a slightly lower value of L and has a shorter period and higher temperature amplitude than that in figure 2(b).

The period is determined by the ratio $\phi \equiv (\bar{C} E_1)/(R c_{w,f} (-\Delta H_1))$, and in general a large value of the numerator (high specific heat and activation energy) corresponds to longer cycling

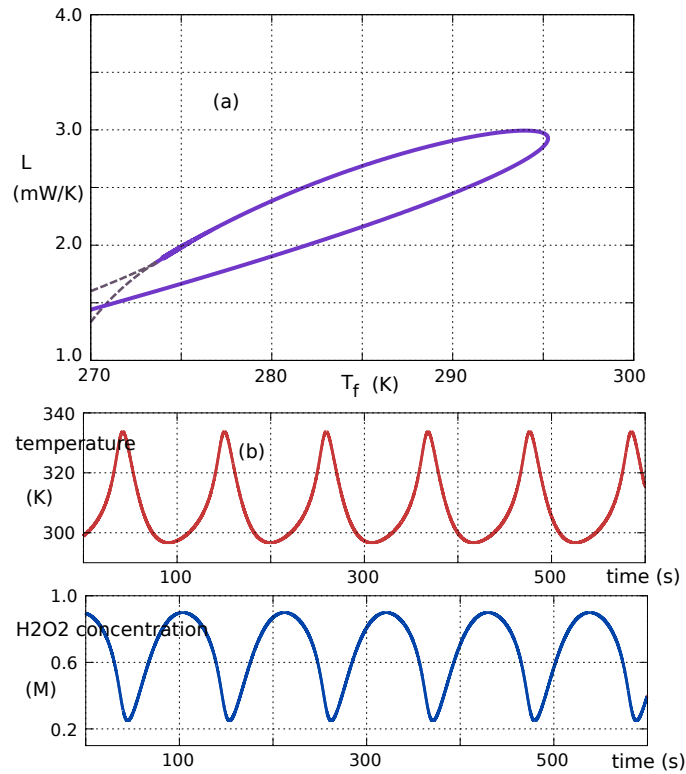


Figure 2. Computed data from equations (1)–(3): (a) Hopf (solid line) and saddle-node (dashed line) bifurcation loci; (b) Time series for $T_f = 282$ K, $L = 2.4$ mW; the oscillation period is 108.7 s. (Online version in colour.)

times and a large value of the denominator (high specific reaction enthalpy) corresponds to shorter period oscillations. The physical parameters V/F (mean residence time), T_f , T_a , and L also affect the period, as might be inferred from the locus of Hopf bifurcations in figure 2(a) [26]. The hydrogen peroxide oscillator has a variable period of the right order — around 80 to 110 seconds — to drive the replication of small RNAs. If the period is too long the RNAs may decay faster than replication can amplify them. If the period is too short the strands do not separate completely and replication may fail.

But the period is not tuned to the putative doubling time for replicant concentration as was the thermal cycling time in [3]. As our system is an open flow system operating at dynamic steady state, where it has ‘forgotten’ the initial conditions, the doubling time is a different quantity from that for the closed batch system in [3]. Here it is defined as a time interval during which the cumulative replicant concentration at the outlet, $c_{xy} + c_z$, becomes equal to twice the inflow concentration $c_{xy,f}$. In equations (1), (2) and (4)–(7) the variables are evolved self-consistently and the doubling time is temperature-dependent, and therefore changes continuously. We can make use of average quantities though.

From computed datafile, the replicant concentration $c_{xy} + c_z$ integrated over one period of 99.3 s (using the trapezoidal rule on 50,000 data points for high accuracy) is 2.281×10^{-5} mol s/l, which yields an instantaneous average concentration $\bar{c}_{xy} + \bar{c}_z = 2.297 \times 10^{-7}$ mol/l and an average doubling time of 0.31 s, for $c_{xy,f} = 3.5 \times 10^{-8}$ M. This does not infer that replication is exponential,

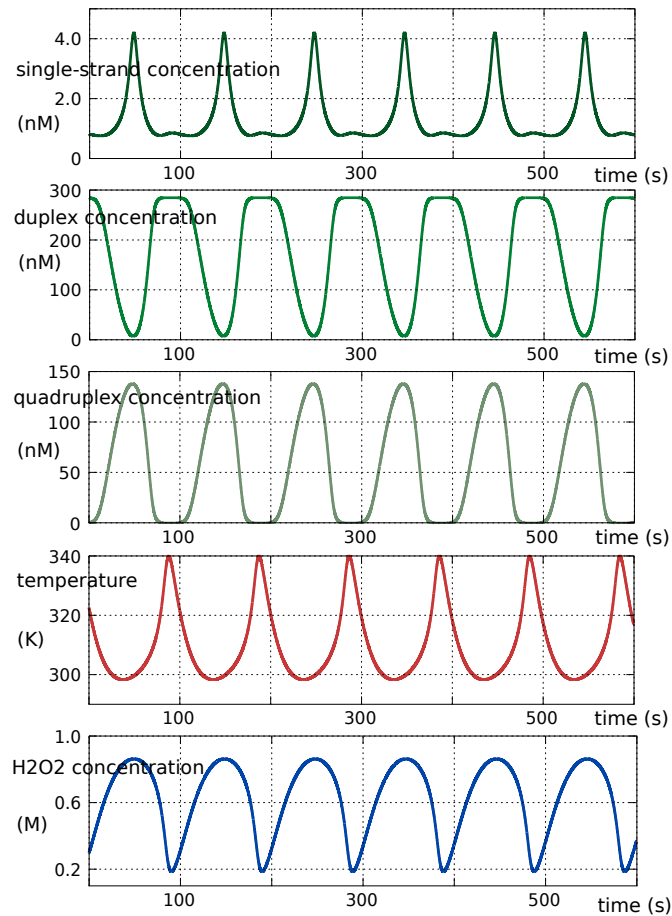


Figure 3. Time series from equations (1), (2) and (4)–(7) for $T_f = 282$ K, $L = 2.3$ mW; period of the oscillation is 99.3 s. (Online version in colour.)

it simply means that on average it takes 0.31 s for the cumulative amount of replicant produced to become equal to twice the feed amount.

Another measure of the system's performance is the ratio $\bar{c}_{xy} + \bar{c}_z / c_{xy,f} = 6.56$. This means the system has been designed so that in steady flow state, for the ideal case where no decay of replicant occurs within the reaction volume, the mean outlet replicant amount is 6.56 times the inlet duplex amount.

Let us consider the phase relationships in figure 3 over one period. Single-strands are consumed as the temperature rises because duplex production by (R3), which requires heat, increases. Correspondingly the concentration of quadruplex falls, almost to zero near the temperature maximum. Single-strands begin to accumulate, but there is only a small bump before quadruplex production picks up as the temperature declines. The presence of this bump means that the oscillation is actually quasiperiodic, and reminds us that the dynamical system of equations (1)–(2) and (4)–(7) is capable of complex periodic and even chaotic behaviour. This may lend additional, powerful capabilities to a molecular replicating system. For example, biperiodic temperature response is capable of replicating two different RNA species, and nature may well have done exactly

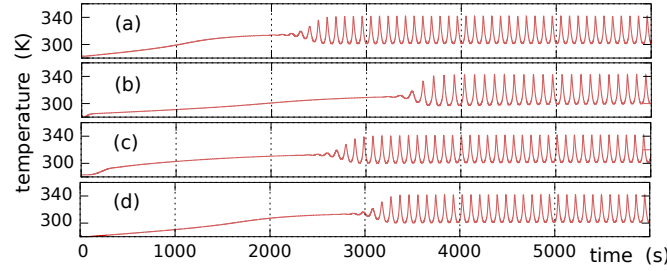


Figure 4. Onset of oscillations via slow drift of parameters. (a) $p \equiv c_{w,f}$, (b) $p \equiv T_a$, (c) $p \equiv F$, (d) both $p_1 \equiv c_{w,f}$ and $p_2 \equiv T_a$. (Online version in colour.)

that in the primordial rock pores. Duplex concentration attains a broad maximum, then declines in phase with the temperature as reaction (R2) is favoured. The inflow delivers more single-strands, which accumulate even though they allow more production of quadruplex.

3.1. Development of self-sustained oscillations

We have addressed also the question of how self-sustained H_2O_2 thermochemical oscillations may have arisen spontaneously in rock pores on the early earth. The fuzzy answer is that parameters may drift quasistatically into an oscillatory régime, such as the loop of Hopf bifurcations in figure 2(a). A precise answer is provided by simulating various scenarios where one or more tunable parameters p in equations 1–3 is given the following increasing time dependence, such that p approaches a constant value:

$$p = p_{\infty} (1 - \alpha \exp(-\gamma t)). \quad (8)$$

A time series from equations (1)–(3) using (8) for one or more parameters is expected to show the temperature increasing slowly, then beginning to wobble, then settling into self-sustained oscillations. Some examples are shown in figure 4. Of course, such evolutions could proceed for millions of years before the onset of periodic behaviour, but we have set the time constant γ in equation (8) more conveniently.

4. Discussion

4.1. Validity and relevance of CSTR paradigm

The CSTR paradigm described by equations (1)–(2) and (4)–(7) can be thought of in two ways.

On the one hand it provides a recipe for a laboratory experiment in a microreactor cell. The flow rate F , inflow concentrations $c_{v,f}$, $c_{w,f}$, $c_{x,f+y,f}$ and $c_{xy,f}$, inflow temperature T_f and wall or ambient temperature T_a are tunable by the experimenter, the wall thermal conductance L and volume V are set by design, and thermokinetic parameters and reaction enthalpies of the RNA reactions can be manipulated by engineering the ribonucleotide sequences and strand lengths. A variety of continuous-flow microreactors are already in use for various calorimetric applications in biotechnology, and the field is developing rapidly [27].

On the other hand we need to address the adequacy of the CSTR as a model for reactions in a porous rock. In an actual physical situation we assume a flow through a porous rock structure

comprising a large array of individual pores, having patterns of connection determined by the character of the rock structure. Provided that the system is sufficiently ergodic, and input flow is steady in volumetric velocity and chemical composition, it is reasonable to assume that the time behaviour in a single pore as reported above gives results at least qualitatively representative of the larger array over times longer than the period of the thermochemical oscillator.

Further, the use of a CSTR model for a pore implicitly assumes a typical residence time \gg the mixing time. Mixing is achieved mainly by convection, and in this respect thermoconvection times of 3–7.5 s were reported by Mast et al. [28]. The mean residence time in our system is 20 s. The perfect mixing assumption is considered to hold adequately when the residence time is around $5\text{--}10 \times$ the mixing time, so the CSTR model can be a reasonably good approximation. The 15 s thermoconvection time reported by Braun and Libchaber [29] is too long for the perfect mixing assumption to hold, and in that case the appropriate model is a system of reaction-convection-diffusion equations and boundary conditions. In that case reactive and convective thermal oscillations would couple in important and interesting ways, but that is for future study. We prefer, at this stage, to avoid the sheer ‘tyranny of numbers’ that still plagues the numerical analysis of such systems, and isolate the reactive thermal oscillations by studying a system for which the perfect mixing assumption holds.

In experiments the mixing behaviour of the system would be characterised by using a tracer to measure the residence time distribution, or by determining the period of time necessary for the system to achieve a desired level of homogeneity. We note that Imai et al. [30] confirmed experimentally the well-stirred condition for a flow microreactor that simulated a hydrothermal environment, in which elongation of oligopeptides was achieved at high temperature and pressure.

4.2. RNA stability to hydrogen peroxide

The response of RNA to H_2O_2 is a mixed story. Some small RNAs have been found to be very stable; for example a 109-nucleotide RNA which is induced by oxidative stress in *E. coli* has an *in vivo* half-life of 12–30 minutes [31]. There is evidence for modern RNA dysfunction, but not degradation, caused by oxidation initiated by H_2O_2 [32]. In [33] it was found that small RNA (~ 50 bases) of yeast is stable to H_2O_2 , but pyrite is reactive in RNA degradation and hydroxyl (OH) radical generation.

Much more is known about the effects of H_2O_2 on DNA, in the context of disease caused by free radical damage. In [34] it was found that 2'-deoxyguanosine was hydroxylated at C-8 when included in the thiosulfate-hydrogen peroxide system. But it is an interesting fact that H_2O_2 does not react directly with DNA, and DNA is not damaged in its presence unless transition metal ions are present [35]. In the presence of transition metal ions OH radicals are generated by the Fenton reaction: $\text{Fe}^{2+} + \text{H}_2\text{O}_2 \rightarrow \text{Fe}^{3+} + \text{OH} + \text{OH}^-$. However, the high and indiscriminate reactivity of the OH radical limits its ability to damage biomolecules, because it is more likely to be scavenged by the iron before attacking DNA or RNA: $\text{OH} + \text{Fe}^{2+} \rightarrow \text{Fe}^{3+} + \text{OH}^-$.

Oxidized RNA evidently may still replicate. For example, oxidized mRNA has been successfully converted to cDNA by reverse transcriptase, with mutations induced in the cDNA by the oxidized RNA bases [36].

In summary, although H_2O_2 may damage or modify RNA (as could many other possible ingredients of primordial soup), there is no reason to suppose that it cannot replicate and pass out

of the reaction zone faster than it is damaged or degraded. RNA that is modified by the action of H_2O_2 in such a way that confers resilience to H_2O_2 damage would, of course, be selected for.

4.3. Occurrence and supply of substrate RNA oligomers

Replication of RNA duplexes by complementary strand pairing raises the thorny question of how such strands could have been produced in the prebiotic primordial soup. It has been shown that 200-mers of RNA can be polymerized and concentrated in a thermal gradient [37], but this does not produce complementary strands preferentially. Polynucleotides > 50 -mers can be synthesized on montmorillonite [38], which also facilitates homochiral selection [39], and this would seem a stronger hypothesis.

A supply of complementary template oligomers could be provided by a variation on the surface-promoted replication procedure in [40], when competitive pathways are included for consumption and production of complementary free RNA species X and Y as indicated in figure 5. Here, too, replication may be driven by an H_2O_2 thermochemical oscillator, because strand separation requires heating and annealing, ligation, and immobilization of single strands is promoted by cooling.

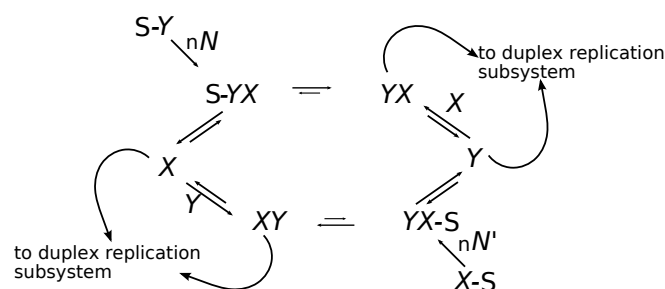


Figure 5. Scheme for supply of template oligomers. The surface-bound single polynucleotide strands $S-X$ and $S-Y$ bind n complementary nucleotide fragments N and N' from solution, which are ligated irreversibly to form $S-XY$ and $S-YX$. Heating promotes release of free X and Y and slower release of duplex XY from S , and melting of free XY to X and Y . The free species can participate in the duplex replication scheme (R2) and (R3).

In another pre-biotic scenario, lipid molecules in a dehydrated environment promoted condensation of nucleic acid monomers, and an alternating wet phase replenished the monomers [41]. Such a system also would be enhanced by the H_2O_2 thermochemical oscillator, which would provide periodic heating to drive the dehydrations and cooling to allow rehydrations.

4.4. Effects of other reactions involving H_2O_2

Hydrogen peroxide may undergo other competing reactions; for example, the Fenton reaction in the presence of $\text{Fe}^{2+}/\text{Fe}^{3+}$ discussed above, which is also exothermic. In this case there would be an extra reaction rate term in the species balance for hydrogen peroxide and in the thermal balance. Such a system has an enhanced propensity towards quasiperiodic oscillations.

It is noteworthy that the Cu(II) -catalysed H_2O_2 /thiosulfate ion reaction displays pH oscillations isothermally [42], implying that the chemistry alone is sufficiently nonlinear to permit oscillatory dynamics, and in any case more complex than (R1) suggests. Spontaneous pH cycling could well

be an assistant driver for RNA replication as it would provide scope for favourable conformation changes.

In summary, we have proposed and explored a previously unrecognized mechanism for driving a replicating system on the prebiotic earth. The chances of a hydrogen peroxide thermochemical oscillator arising spontaneously on the early earth in the presence of nucleotide precursors are perhaps very small. However, the earth is large, rock pores are innumerable, and there was plenty of time on the early earth for improbable events to happen.

Braun and Libchaber [29] are strong proponents of an interdisciplinary approach between biochemistry and geophysics for understanding the origin of life at the molecular level. We have added some insights that originated in chemical engineering, showing that an interdisciplinary approach is indeed fruitful.

Table 2. Nomenclature and numerical values.

Symbol (units), definition	Quantity	Values	
		no RNA	with RNA
A ($M^{n-1}s^{-1}$), pre-exponential factor	A_1	1.63×10^{10}	1.63×10^{10}
	A_2	n/a	1.69×10^{12}
	A_3	n/a	1.0×10^{39}
c (M), concentration	$c_{v,f}$	0.9	0.9
	$c_{w,f}$	1.35	1.35
	$c_{x,f+y,f}$	0	5.0×10^{-7}
	$c_{xy,f}$	0	3.5×10^{-8}
\bar{C} ($J K^{-1}$), volumetric specific heat	\bar{C}	3400	3400
E ($kJ mol^{-1}$), activation energies	E_1	68.12	68.12
	E_2	n/a	-10
	E_3	n/a	260.14
F ($\mu l s^{-1}$), flow rate	F	0.50	0.50
ΔH ($kJ mol^{-1}$), reaction enthalpies	ΔH_1	-612.5	-612.5
	ΔH_2	n/a	-169.6
	ΔH_3	n/a	260.14
L ($W K^{-1}$), wall thermal conductance			
n , sum of species reaction orders			
T (K), temperature	T_a	283	283
V (μl) pore volume	V	10.0	10.0
Subscripts			
1, 2, 3	pertaining to (R1), (R2), (R3)		
a	of the ambient or wall temperature		
f	of the flow		
v, w	of thiosulfate, H_2O_2		
x, y, z	of single-strands, duplex, quadruplex		

Appendix: Choices of numerical values

- The weighted average volumetric specific heat $\bar{C} = 3400 \text{ J K}^{-1} \text{ l}^{-1}$ is considerably lower than that of pure water. The volumetric specific heat of sea water is about $3850 \text{ J K}^{-1} \text{ l}^{-1}$ and that of H_2O_2 is about $2620 \text{ J K}^{-1} \text{ l}^{-1}$, from which we arrive at the given value of $3400 \text{ J K}^{-1} \text{ l}^{-1}$.
- The activation energies and pre-exponential factors of the RNA reactions were obtained from the data in [3] using

$$E = \frac{R \ln (k(T_2) / k(T_1))}{1/T_1 - 1/T_2}$$

then $A = k \exp(E/RT)$. The activation energy for the association reaction (R2) is zero in [3] but we used the small negative value of 10 kJ/mol in the calculations to reflect the fact that the rates of association reactions of biological macromolecules often decrease with temperature, because due to thermal motion a smaller fraction of energetically favourable collisions result in reaction. The data in [3] gave a pre-exponential factor for reaction (R3) in the main article of 10^{45} s^{-1} . On the basis of only two data points this should not be taken too literally; in practice we had to reduce it to 10^{39} s^{-1} to couple the reaction to the thermochemical oscillator.

Acknowledgement: Rowena Ball is recipient of Australian Research Council Future Fellowship FT0991007.

References

- [1] Neveu M, Kim H-J, Benner SA. 2013 The “strong” RNA world hypothesis: Fifty years old. *Astrobiol.* **13** 391–403. (DOI 10.1089/ast.2012.0868)
- [2] Kováč L, Nosek J, Tomáška L. 2003 An overlooked riddle of life’s origins: Energy-dependent nucleic acid unzipping. *J. Mol. Evol.* **57** S182–S189. (DOI 10.1007/s00239-003-0026-z)
- [3] Krammer H, Möller FM, Braun D. 2012 Thermal, autonomous replicator made from transfer RNA. *Phys. Rev. Lett.* **108** 238104. (DOI 10.1103/PhysRevLett.108.238104)
- [4] Braun D, Goddard NL, Libchaber A. 2003 Exponential DNA replication by laminar convection. *Phys. Rev. Lett.* **91** 158103. (DOI 10.1103/PhysRevLett.91.158103)
- [5] Matatov YI. 1980 Study of the abiotic synthesis of amino acids during the polycondensation of formaldehyde and hydroxylamine. (In Russian with English abstract.) *Z. Evol. Bio. Fiz.* **16** 189–193.
- [6] Ramirez WF, Turner BA. 1969 The dynamic modeling, stability, and control of a continuous stirred tank reactor. *AIChE J.* **15** 853–860. (DOI 10.1002/aic.690150611)
- [7] Chang M, Schmitz RA. 1975 An experimental study of oscillatory states in a stirred reactor. *Chem. Eng. Sci.* **30** 21–34. (DOI 10.1016/0009-2509(75)85112-8)
- [8] Wirges HP. 1980 Experimental study of self-sustained oscillations in a stirred tank reactor. *Chem. Eng. Sci.* **35** 2141–2146. (DOI 10.1016/0009-2509(80)85038-X)
- [9] Zeyer KP, Mangold M, Obertopp T, Gilles ED. 1999 The iron (III)- catalysed oxidation of ethanol by hydrogen peroxide: A thermokinetic oscillator. *J. Phys. Chem. A* **103** 5515–5522. (DOI 10.1021/jp990710v)
- [10] Ball R. 2013 Thermal oscillations in the decomposition of organic peroxides: identification of a hazard, use, and suppression. *Ind. Eng. Chem. Res.* **52** 922–933. (DOI 10.1021/ie301070d)
- [11] Cohen WC, Spencer JL. 1962 Determination of chemical kinetics by calorimetry. *Chem. Eng. Progr.* **58** (12) 40–41.
- [12] Lo SN, Cholette A. 1972 Experimental study on the optimum performance of an adiabatic MT reactor. *Can. J. Chem. Eng.* **50** 71–80. (DOI 10.1002/cjce.5450500113)
- [13] Williams RD. 1974 Indirect measurement of reaction rate. *Chem. Eng. Ed.* **VIII** (1) 28–30.
- [14] Guha BK, Narsimham G, Agnew JB. 1975 An experimental study of transient behavior of an adiabatic continuous-flow stirred tank reactor. *Ind. Eng. Chem. Process Des. Dev.* **14** 146–152. (DOI 10.1021/i260054a009)
- [15] Lin KF, Wu LL. 1981 Performance of an adiabatic controlled cycled stirred tank reactor. *Chem. Eng. Sci.* **36** 435–444. (DOI 10.1016/0009-2509(81)85026-9)
- [16] Grau MD, Nogués JM, Puigjaner L. 2000 Batch and semibatch reactor performance for an exothermic reaction. *Chem. Eng. Process.* **39** 141–148. (DOI 10.1016/0009-2509(81)85026-9)
- [17] Tang BL. 2007 Emergence of life — how and where? An update based on recent ideas. *Prog. Nat. Sci.* **17** 500–510. (DOI 10.1080/10020070708541029)
- [18] Foustoukos DI, Houghton JL, Seyfried Jr WE, Sievert SM, Cody GD. 2011 Kinetics of H₂–O₂–H₂O redox equilibria and formation of metastable H₂O₂ under low temperature hydrothermal conditions. *Geochim. Cosmochim. Acta* **75** 1594–1607. (DOI 10.1016/j.gca.2010.12.020)
- [19] Borda MJ, Elsetinow AR, Schoonen MA, Strongin DR. 2001 Pyrite-induced hydrogen peroxide formation as a driving force in the evolution of photosynthetic organisms on an early earth. *Astrobiol.* **1** 283–288. (DOI 10.1089/15311070152757474)
- [20] Borda MJ, Elsetinow AR, Strongin DR, Schoonen MA. 2003 A mechanism for the production of hydroxyl radical at surface defect sites on pyrite. *Geochim. Cosmochim. Acta* **67** (2003) 935–939. (DOI 10.1016/S0016-7037(02)01222-X)
- [21] Pugh CE, Hossner LR, Dixon JB. 1981 Pyrite and marcasite surface area as influenced by morphology and particle diameter. *Soil Sci. Soc. Am. J.* **45** 979–982. (DOI 10.2136/sssaj1981.03615995004500050033x)
- [22] Barrie CT, Hannington MD. 1999 Classification of volcanic-associated massive sulfide deposits on host-rock composition. *Rev. Econ. Geol.* **8** 325–356.
- [23] Barbusiński K. 2009 Fenton reaction — controversy concerning the chemistry. *Ecol. Chem. Eng. S* **16** 347–358.
- [24] Xu Y, Schoonen MAA, Nordstrom DK, Cunningham KM, Ball JW. 1998 Sulfur geochemistry of hydrothermal

- waters in Yellowstone National Park: I. the origin of thiosulfate in hot spring waters. *Geochim. Cosmochim. Acta* **62** 3729–3743. (DOI 10.1016/S0016-7037(98)00269-5)
- [25] von Kiedrowski G, Szathmáry E. 2001 Selection versus coexistence of parabolic replicators spreading on surfaces. *Selection* **1** 173–180. (DOI 10.1556/Select.1.2000.1-3.17)
 - [26] Gray P, Scott SK. 1994. Chemical Oscillations and Instabilities: Non-linear Chemical Kinetics. Clarendon Press.
 - [27] Carreto-Vazquez VH, Liu Y-S, Bukur DB, Mannan MS. 2011 Chip-scale calorimeters: Potential uses in chemical engineering. *J. Loss Prevent. Process Ind.* **24** 34–42. (DOI 10.1016/j.jlp.2010.07.012)
 - [28] Mast CB, Osterman N, Braun D. 2012 Thermal solutions for molecular evolution. *Int. J. Mod. Phys. B* **26** 1230017–1–13. (DOI 10.1142/S0217979212300174)
 - [29] Braun D, Libchaber A. 2004 Thermal force approach to molecular evolution. *Phys. Biol.* **1** 1–8. (DOI 10.1088/1478-3967/1/1/P01)
 - [30] Imai E, Honda H, Hatori K, Brack A. 1991 Elongation of oligopeptides in a simulated hydrothermal system. *Science* **283** 831–833. (DOI 10.1126/science.283.5403.831)
 - [31] Altuvia S, Weinstein-Fischer D, Zhang A, Postow L, Storz G. 1997 A small, stable RNA induced by oxidative stress: Role as a pleiotropic regulator and antimutator. *Cell* **90** 43–53. (DOI 10.1016/S0092-8674(00)80312-8)
 - [32] Liu M, Gong X, Alluri RK, Wu J, Sablo T, Li Z. 2012 Characterization of RNA damage under oxidative stress in *Escherichia coli*. *Biol. Chem.* **393** 123–132. (DOI 10.1515/hsz-2011-0247)
 - [33] Cohn CA, Laffers R, Schoonen MA. 2006 Using yeast RNA as a probe for generation of hydroxyl radicals by earth materials. *Environ. Sci. Technol.* **40** 2838–2843. (DOI 10.1021/es052301k)
 - [34] Seto H, Koike H, Sasano H. 1994 Hydroxylation of deoxyguanosine at the C-8 position in the thiosulfate-hydrogen peroxide reaction system. Evidence of hydroxyl radical generation in the system. *Chem. Lett.* **23** 993–996. (DOI 10.1246/cl.1994.993)
 - [35] Halliwell B, Aruoma OI. 1991 DNA damage by oxygen-derived species — its mechanism and measurement in mammalian systems. *FEBS Lett.* **281** 9–19. (DOI 10.1016/0014-5793(91)80347-6)
 - [36] Kamiya H, Suzuki A, Kawai K, Kasai H, Harashima, H. 2007 Effects of 8-hydroxy-GTP and 2-hydroxy-ATP on in vitro transcription. *Free Radical Biology and Medicine* **43** 837–843. (DOI 10.1016/j.freeradbiomed.2007.05.034)
 - [37] Mast CB, Schink S, Gerland U, Braun D. 2013 Escalation of polymerization in a thermal gradient. *Proc. Nat. Acad. Sci. USA* **110** 8030–8035. (DOI 10.1073/pnas.1303222110)
 - [38] Ferris JP, Hill AR, Liu RH, Orgel LE. 1996 Synthesis of long prebiotic oligomers on mineral surfaces. *Nature* **381** (6577) 59–61. (DOI 10.1038/381059a0)
 - [39] Joshi PC, Aldersley MF, J. P. Ferris JP. 2013 Progress in demonstrating homochiral selection in prebiotic RNA synthesis. *Adv. Space Res.* **51** 772–779. (DOI 10.1016/j.asr.2012.09.036)
 - [40] Luther A, Brandsch R, von Kiedrowski G. 1998 Surface-promoted replication and exponential amplification of DNA analogues. *Nature* **396** 245–248. (DOI 10.1038/24343)
 - [41] Olasagasti F, Hyunsung JK, Pourmand N, Deamer DW. 2011 Non-enzymatic transfer of sequence information under plausible prebiotic conditions. *Biochimie* **93** 556–561. (DOI 10.1016/j.biochi.2010.11.012)
 - [42] Orbán M, Epstein IR. 1987 Chemical oscillators in group VIA: the copper(II)-catalyzed reaction between hydrogen peroxide and thiosulfate ion. *J. Am. Chem. Soc.* **109** 101–106. (DOI 10.1021/ja00235a017)

Figure captions and short title for page headings

Figure 1. The quadruplex RNA species Z . The duplex replicator species are XY and xy , which for the purposes of the simulation are equivalent. See ref. [3] for more details. (Online version in colour.)

Figure 2. Computed data from equations (1)–(3): (a) Hopf (solid line) and saddle-node (dashed line) bifurcation loci; (b) Time series for $T_f = 282$ K, $L = 2.4$ mW; the oscillation period is 108.7 s. (Online version in colour.)

Figure 3. Time series from equations (1), (2) and (4)–(7) for $T_f = 282$ K, $L = 2.3$ mW; period of the oscillation is 99.3 s. (Online version in colour.)

Figure 4. Onset of oscillations via slow drift of parameters. (a) $p \equiv c_{w,f}$, (b) $p \equiv T_a$, (c) $p \equiv F$, (d) both $p_1 \equiv c_{w,f}$ and $p_2 \equiv T_a$. (Online version in colour.)

Figure 5. Scheme for supply of template oligomers. The surface-bound single polynucleotide strands $S-X$ and $S-Y$ bind n complementary nucleotide fragments N and N' from solution, which are ligated irreversibly to form $S-XY$ and $S-YX$. Heating promotes release of free X and Y and slower release of duplex XY from S , and melting of free XY to X and Y . The free species can participate in the duplex replication scheme (R2) and (R3).

Short title: Primordial RNA replication